

NASA  
TP  
1787  
c.1

# NASA Technical Paper 1787

LOAN COPY: RE  
AFWL TECHNICAL  
KIRTLAND AFB,

0067734



TECH LIBRARY KAFB, NM

## A Study of the Sonic-Boom Characteristics of a Blunt Body at a Mach Number of 6

George C. Ashby, Jr.

DECEMBER 1980

**NASA**



NASA Technical Paper 1787

A Study of the Sonic-Boom  
Characteristics of a Blunt  
Body at a Mach Number of 6

George C. Ashby, Jr.  
*Langley Research Center  
Hampton, Virginia*



National Aeronautics  
and Space Administration

**Scientific and Technical  
Information Branch**

1980

## SUMMARY

The sonic-boom pressure signatures parallel to the axis of a blunt body were measured at several fixed distances from the axis at Mach 6. A finite-difference computer program was shown to give reasonable estimates of the pressure signatures.

The computed near-field static-pressure signature (2 model lengths from axis) was extrapolated to the far field by a program using the method of characteristics. The peak overpressure of the extrapolated signature agrees with that predicted by linearized far-field sonic-boom theory and provides some verification of the usefulness of the latter theory in predicting the ground level overpressures at Mach numbers at least as high as 6.

## INTRODUCTION

The nature of sonic-boom phenomena has been investigated extensively, and theories have been developed to provide accurate estimates of the sonic-boom characteristics for a wide variety of bodies, wings, wing-body combinations, and complete supersonic aircraft configurations. Reference 1 gives a bibliography of these investigations and examines the applicability of linearized far-field sonic-boom theory to very blunt body shapes, which are representative of entry vehicles and bodies with extensive exhaust gas plumes in supersonic flight.

Reference 1 points out that, generally, the studies in the bibliography and its own blunt-body investigation results have demonstrated a remarkable ability for simplified theoretical methods to provide accurate estimates of the sonic-boom characteristics at large propagation distances relative to the body dimensions. Appropriate to these observations, the senior investigator of reference 1 developed a simplified technique to calculate the sonic-boom characteristics, of greatest interest, for a wide variety of airplane configurations and spacecraft (ref. 2).

In the investigation of reference 1, static-pressure signatures generated by a paraboloid of revolution were measured at distances from the body axis of 2 to 32 body lengths at Mach 4.14. The peak overpressures of the signatures were shown to decay with distance from the body, and approach the linearized theoretical far-field value as a limit.

The current study was conducted to extend the investigation of the applicability of linearized far-field sonic-boom theory to blunt bodies from Mach 4.14 to Mach 6. Static pressure signatures were measured at Mach 6 about the same paraboloid of revolution and at the same distances from the body axis as were measured at Mach 4.14 (ref. 1). However, because of the tunnel and probe traverse mechanism limitations, the measured signatures at Mach 6 were not complete at all the stations from 2 to 32 body lengths from the axis. To

obtain good estimates of the true signatures at Mach 6, the finite difference computer programs of references 3 and 4 were first shown to give reasonably good estimates of the signatures at Mach 4.14, and then were used with confidence at Mach 6 along with the limited pressure measurements to establish a complete set of signatures. The variation of these signatures with distance from the body, along with the signature obtained by extrapolating a computed near-field signature to the far field (via a program using the method of characteristics), was used to evaluate the applicability of the signature estimated by the far-field sonic-boom theory.

The purposes of this report are to: (1) demonstrate that the finite-difference programs can reasonably predict the sonic-boom signatures in the near field of a very blunt body (diameter to length ratio of 2.0) at Mach numbers up to 6; (2) to show that the overpressure predicting capability of linearized far-field theory can be extended from Mach 4.14 to at least Mach 6; and (3) to demonstrate the capabilities of a computer program (method of characteristics) to extrapolate the near-field signature of a blunt body to the far field at Mach numbers up to 6.

This report presents the comparisons between the measured and calculated signatures for both Mach 4.14 and Mach 6. Composite plots of computed and extrapolated signatures, and plots of signature parameters used to evaluate the linearized far-field sonic-boom theory are also presented for both Mach numbers.

#### SYMBOLS

D	body maximum diameter, base diameter, cm
h	distance from flight path to pressure probes, cm
$K_r$	reflection factor, 1.0 for this report
l	reference length of configuration, cm (see fig. 1)
$M_2$	Mach number behind bow shock
$M_\infty$	free-stream Mach number
p	local static pressure, Pa
$\Delta p$	sonic-boom overpressure, $p - p_\infty$ , Pa
$\Delta p_A$	adjusted incremental pressure at bow shock of measured signature (see fig. 6)
$\Delta p_b$	incremental pressure at bow shock of theoretical pressure signature
$P_{t,2}$	total pressure behind bow shock, Pa
$P_{t,3}$	pitot pressure behind bow shock, Pa

$P_{t,\infty}$	free-stream total pressure, Pa
$P_{t,\infty}^*$	free-stream pitot pressure, Pa
$P_2$	static pressure behind bow shock, Pa
$P_\infty$	free-stream static pressure, Pa
$r$	body radius, cm
$x$	distance measured along body longitudinal axis from body nose, cm
$\Delta x$	longitudinal distance from point on pressure signature to point where pressure signature curve crosses zero overpressure reference axis, cm
$\Delta x_A$	adjusted value of length of positive portion of measured pressure signature (see fig. 6)
$\Delta x_b$	length of positive portion of theoretical pressure signature
$\beta$	$= \sqrt{M_\infty^2 - 1}$
$\theta$	shock-wave angle, deg

## APPARATUS AND TESTS

### Tunnel

The tests for this report were conducted in the Langley 20-Inch Mach 6 Tunnel at an average stagnation pressure of 2.86 MPa and an average stagnation temperature of 494 K. Operational characteristics of the facility and the flow calibration are presented in reference 5.

### Models and Instrumentation

The two models used in the test program (fig. 1), the same models used in reference 1, had identical forebody shapes but differed in size by a scale factor of 4. The large model was used to measure pressure signatures at nondimensionalized distances of 2, 4, and 8; and the small model was used for nondimensionalized distances of 8, 16, and 32 (the same values of  $h/l$  that were used at Mach 4.14). The model forebodies are paraboloids defined by the equations shown in figure 1. Electrical transducers were used to sense the pressures, and a digital shaft encoder was used to identify the position of the probe in the flow field. The pitot-pressure probe (fig. 1) had an internal bevel to reduce the probe sensitivity to flow angle.

## Tests and Methods

The pitot-pressure probes and models were mounted in the Mach 6 test section as shown in figure 2. Pitot-pressure measurements were made at stations from in front of the bow shock to the downstream limit of the traverse apparatus. For each run, the probe was set in the most forward survey position at the distance  $h$  from the reference axis. The model was positioned longitudinally so that the bow shock was slightly aft of the nose of the probe. At the beginning of each run, the probe was moved aft until the beginning of the sharp pressure increase at the shock was encountered. The probe was then moved forward of the shock and the data traverse across the shock was begun. Discrete data points were taken over the allowable traverse distance with multiple data points being taken in the vicinity of maximum overpressure to define that particular point as accurately as possible. Figure 3, taken from reference 1, gives a perspective of how the pressure signature varies with distance  $h$  from the model longitudinal axis.

Initially, a static-pressure probe (ref. 6) was used simultaneously with the pitot-pressure probe to measure the static pressures; subsequently, the static-pressure probe was discovered to be too long and the length of travel of the traverse mechanism too short for the probe to measure pressures free of shock interference. Therefore, data from this probe are not presented in this report.

At the outer measuring station ( $h/l = 8$  for the large model and  $h/l = 32$  for the small model) the pitot-pressure probe was in the tunnel wall boundary layer, and only the measurements at  $h/l = 2$  and  $4$  for the large model and  $h/l = 8$  and  $16$  for the small model are considered. The limit of travel of the traverse mechanism also prevented full signature measurements by the pitot-pressure probe at some stations. Enough of the signature was measured, however, to permit analyses and comparisons to be made.

## DATA REDUCTION

The Mach 4.14 data were obtained from reference 1 wherein the pressure signatures were measured using a static-pressure probe. For the Mach 6 tests, the free-stream Mach number  $M_\infty$  and static pressure  $p_\infty$  were obtained by using the free-stream pitot pressure  $p_{t,\infty}$  from the floor-mounted pitot probe and the free-stream total pressure  $p'_{t,\infty}$ . The static-pressure signatures from the pitot probe were calculated iteratively with the following equations (ref. 7):

From oblique-shock relationships,

$$\frac{p_{t,2}}{p_{t,\infty}} = \left( \frac{6M_\infty^2 \sin^2 \theta}{M_\infty^2 \sin^2 \theta + 5} \right)^{7/2} \left( \frac{6}{7M_\infty^2 \sin^2 \theta - 1} \right)^{5/2} \quad (1)$$

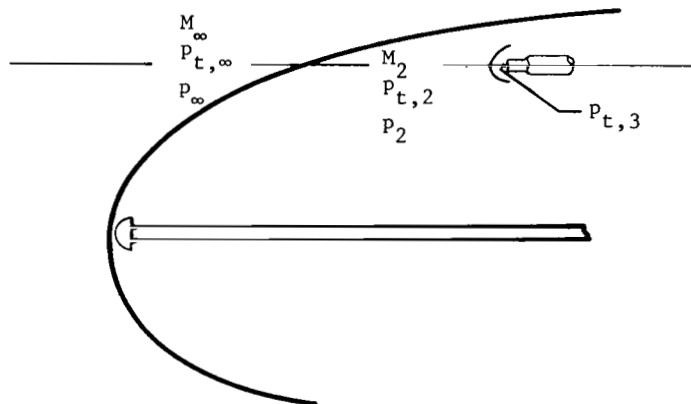
$$M_2^2 = \frac{36M_\infty^4 \sin^2 \theta - 5(M_\infty^2 \sin^2 \theta - 1)(7M_\infty^2 \sin^2 \theta + 5)}{(7M_\infty^2 \sin^2 \theta - 1)(M_\infty^2 \sin^2 \theta + 5)} \quad (2)$$

From normal-shock relationships,

$$\frac{p_{t,3}}{p_{t,2}} = \left( \frac{6M_2^2}{M_2^2 + 5} \right)^{7/2} \left( \frac{6}{7M_2^2 - 1} \right)^{5/2} \quad (3)$$

From one-dimensional isentropic flow relationships,

$$\frac{p_2}{p_{t,2}} = \left( 1 + \frac{M_2^2}{5} \right)^{-7/2} \quad (4)$$



A shock angle  $\theta$  was assumed, and initial values for  $p_{t,2}$  and  $M_2$  were computed from equations (1) and (2). The computed value of  $M_2$  and the measured pitot pressure  $p_{t,3}$  were used in equation (3) to determine another value for  $p_{t,2}$ . The series of calculations was repeated with different shock angles until the two values of  $p_{t,2}$  converged. After convergence was obtained, equation (4) was used to calculate  $p_2$ .

This type of calculation, wherein  $p_{t,3}$  is the only known quantity behind the shock, is valid only near the shock. As the probe moves aft from the bow shock,  $M_2$  is not constant along the path from the shock to the probe and this method does not give a unique solution for  $M_2$ ,  $p_{t,2}$ , or  $p_2$ . The accuracy of the calculated static pressure decreases directly with probe distance behind the shock, but the decrease is dependent on the shock curvature in the vicinity of the path. Nonetheless, the correct value of  $p_2$  at the shock establishes the peak overpressure, and the remainder of the values computed from the pitot pressure are useful for establishing the signature curves.

## RESULTS AND DISCUSSIONS

The applicability of the linearized far-field sonic-boom theory at Mach numbers higher than 4.14 was evaluated by comparing its signature with the far-field signature which was an extrapolation of the predicted near-field signature at Mach 6. The finite-difference computer programs of references 3 and 4 were used to calculate the theoretical signatures at Mach 4.14 as well as Mach 6. As will shortly be shown, there was favorable agreement between the predicted and the measured signatures at Mach 4.14. This favorable agreement was the basis for confidence in using the programs to predict signatures at Mach 6 for analysis and comparison with wind tunnel data.

The calculated signatures at Mach 4.14 are compared with the measured signatures from reference 1 in figure 4 at  $h/l = 2, 4, 8, 16,$  and  $32$ . The signature lengths are in good agreement at all stations, and the agreement between the peak overpressures improves as distance from the model increases, becoming practically coincident at  $h/l = 32$ . As pointed out in reference 1, the probe used in that investigation was not expected to measure the correct pressure near strong shocks. That fact, coupled with good agreement between the two signatures at distances greater than  $h/l = 8$  indicates that the finite difference code is a viable method for determining the pressure signatures about blunt bodies at Mach 4.14. Trusting that the program would perform equally well at Mach 6.0, signatures were calculated and compared with wind tunnel data.

The calculated pressure signatures for Mach 6 are presented along with the pressures obtained from the pitot-pressure measurements in figure 5. The pressures from the pitot-probe measurements are accurate the the shock (see "Data Reduction"); so, the measured and calculated signatures were aligned in the peak overpressure region using the relative location of the signatures at Mach 4.14 (fig. 4) as a guide. To aid in the comparative analysis of the calculated and measured signatures, the measured signatures were adjusted near the shock by the method outlined in reference 8. The adjusted peak overpressures for the measured data are seen to be in reasonably good agreement with the calculated values; but the measured signature lengths are short, especially at the station nearest the body. These results for Mach 6 are more clearly depicted in figure 6 where the adjusted measurements of peak overpressures and signature lengths are divided by the calculated values for both Mach 6 and Mach 4.14. The data for both Mach numbers are presented to obtain a critical assessment of the capabilities of the finite-difference computer programs. The good agreement at Mach 4.14 between the calculated and measured signature length, at all measuring stations, and the progressively improving agreement of the peak overpressures with distance from the body (coupled with the good agreement at Mach 6 between the calculated and adjusted measured peak overpressures at all measuring stations), indicate that the prediction capability of the programs is very good.

The results of reference 1 have indicated that the linearized far-field sonic-boom theory is applicable for blunt bodies at Mach 4.14. To extend the assessment to Mach 6, the calculated signatures in terms of correlating pressure and length parameters are presented in figure 7. These parameters (listed



below) were formulated in reference 9 and were applied to the body shape of this investigation in reference 1.

$$\frac{\Delta p_b}{p} \left( \frac{h}{l} \right)^{3/4} = \kappa_r \beta^{1/4} (0.537) \frac{D}{l}$$

$$\frac{\Delta x_b}{l} \left( \frac{h}{l} \right)^{-1/4} = \frac{M_\infty^2}{\beta^{3/4}} (0.921) \frac{D}{l}$$

Through the use of these parameters, theoretical signatures for a given body and Mach number may be represented in the far field by a simple "N wave." (See ref. 1.) By plotting the downstream zero overpressure points at a common origin, the pressure signatures calculated by the finite-difference method are shown to evolve toward the far-field theoretical signature as  $h/l$  increases. Also shown on the plot are the extrapolations from  $h/l = 2.0$  of the finite-difference signature using the method of characteristics program of reference 10. This method of extrapolation appears to approach a limiting signature that has about the same overpressure but is somewhat shorter in length than the linearized far-field theoretical signature. The validity of this limiting

signature becomes apparent when the overpressure  $\left( \frac{\Delta p}{p_\infty} \left( \frac{h}{l} \right)^{3/4} \right)$  and length  $\left( \frac{\Delta x}{l} \left( \frac{h}{l} \right)^{-1/4} \right)$  parameters and the impulse (area under the positive portion of the signature) are plotted as a function of  $h/l$  ( $\log_2$  of  $h/l$ ) in figure 8. The three curves fair asymptotically in a smooth manner to the limits set by the extrapolation method at approximately the same  $h/l$  location; whereas, the length parameter and impulse curves (figs. 8(b) and 8(c)) would be smoothly asymptotic to the linearized far-field theory limit at a greater  $h/l$  location.

In reference 1, the experimental data at Mach 4.14 were analyzed to indicate the rate at which far-field conditions were being approached. The overpredictions of signature length and impulse by the linearized far-field theory were also observed but were not attributed to signature length error (fig. 6, ref. 1). Since the analytic programs were shown to be useful for the Mach 6 data, they were applied to the Mach 4.14 data and are presented in figures 9 and 10 of this report. Results similar to those at Mach 6 were obtained. The peak overpressures, signature lengths, and impulse fair asymptotically in a smooth manner to the limits set by the extrapolation method at approximately the same  $h/l$  locations.

## CONCLUDING REMARKS

The sonic-boom pressure signatures parallel to the axis of a blunt body were measured at several fixed distances from the axis at Mach 6. A finite-difference computer program was used to compute the signatures at Mach numbers 4.14 and 6 for comparison with experimental data at the two Mach numbers. Analysis of these data show that finite-difference computer programs can be used to obtain reasonable estimates of the pressure signatures about bodies of revolution with a ratio of diameter to length of 2 at Mach numbers at least as high as 6.0.

The computed near-field static-pressure signature was extrapolated by a program using the method of characteristics. A comparison of this extrapolated signature with the signature predicted by the linearized far-field sonic-boom theory shows that the peak overpressures are about the same, but the far-field theory overestimates the signature length. These results show that linearized far-field sonic-boom theory can be used to estimate the ground level overpressures from blunt bodies flying at Mach numbers at least as high as 6.

Langley Research Center  
National Aeronautics and Space Administration  
Hampton, VA 23665  
December 2, 1980

#### REFERENCES

1. Carlson, Harry W.; and Mack, Robert J.: A Study of The Sonic-Boom Characteristics of a Blunt Body at a Mach Number of 4.14. NASA TP-1015, 1977.
2. Carlson, Harry W.: Simplified Sonic-Boom Prediction. NASA TP-1122, 1978.
3. Marconi, Frank; Salas, Manuel; and Yaeger, Larry: Development of a Computer Code for Calculating the Steady Super/Hypersonic Inviscid Flow Around Real Configurations. Volume I - Computational Technique. NASA CR-2675, 1976.
4. Marconi, Frank; and Yaeger, Larry: Development of a Computer Code for Calculating the Steady Super/Hypersonic Inviscid Flow Around Real Configurations. Volume II - Code Description. NASA CR-2676, 1976.
5. Goldberg, Theodore J.; and Hefner, Jerry N. (appendix by James C. Emery): Starting Phenomena for Hypersonic Inlets With Thick Turbulent Boundary Layers at Mach 6. NASA TN D-6280, 1971.
6. Ashby, George C., Jr.: Near-Field Sonic-Boom Pressure Signatures for the Space Shuttle Launch and Orbiter Vehicles at Mach 6. NASA TP-1405, 1979.
7. Ames Research Staff: Equations, Tables, and Charts for Compressible Flow. NACA Rep. 1135, 1953. (Supersedes NACA TN 1428.)
8. Carlson, Harry W.: Correlation of Sonic-Boom Theory With Wind-Tunnel and Flight Measurements. NASA TR R-213, 1964.
9. Walkden, F.: The Shock Pattern of a Wing-Body Combination, Far From the Flight Path. Aeronaut. Q., vol. IX, pt. 2, May 1958, pp. 164-194.
10. Ferri, A.; Ting, L.; and Lo, R. W.: Nonlinear Sonic Boom Analysis Including the Asymmetric Effects. AIAA Paper No. 76-587, July 1976.

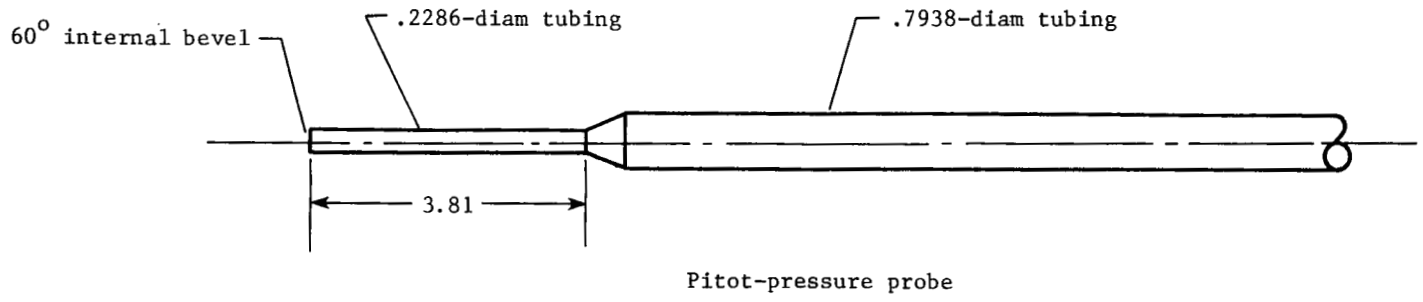
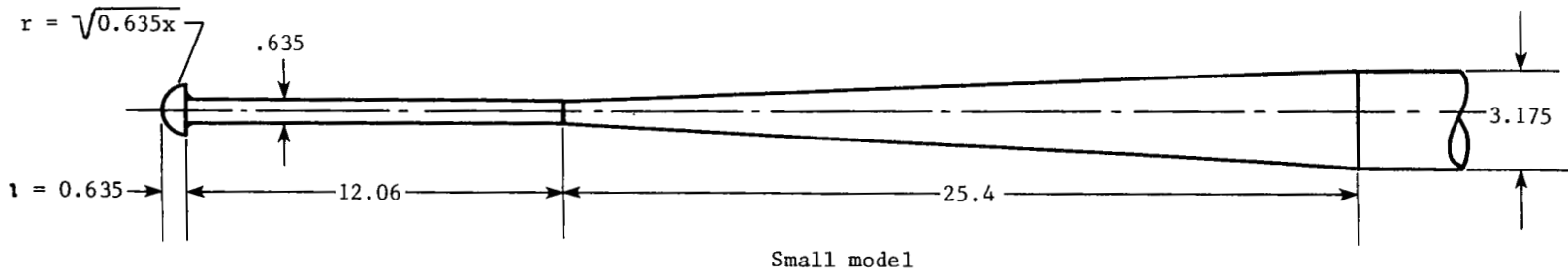
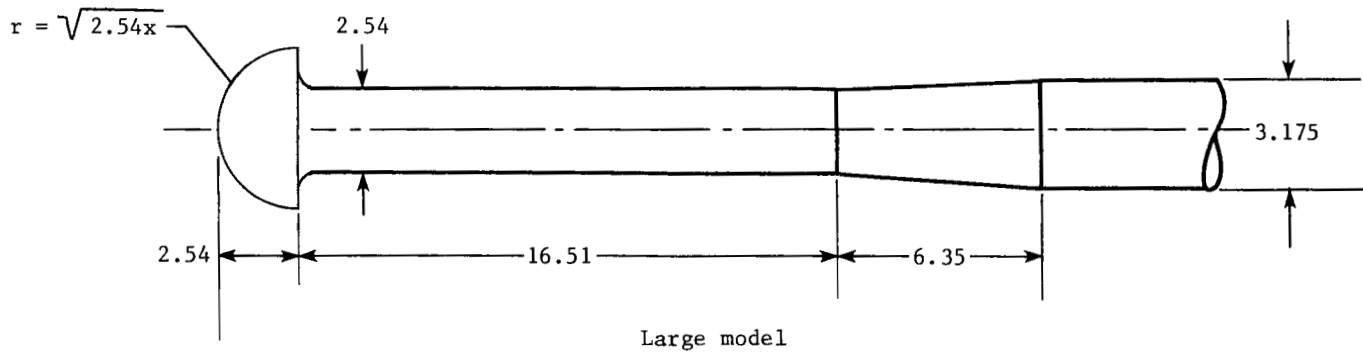


Figure 1.- Models and traverse probe. All dimensions are in cm.

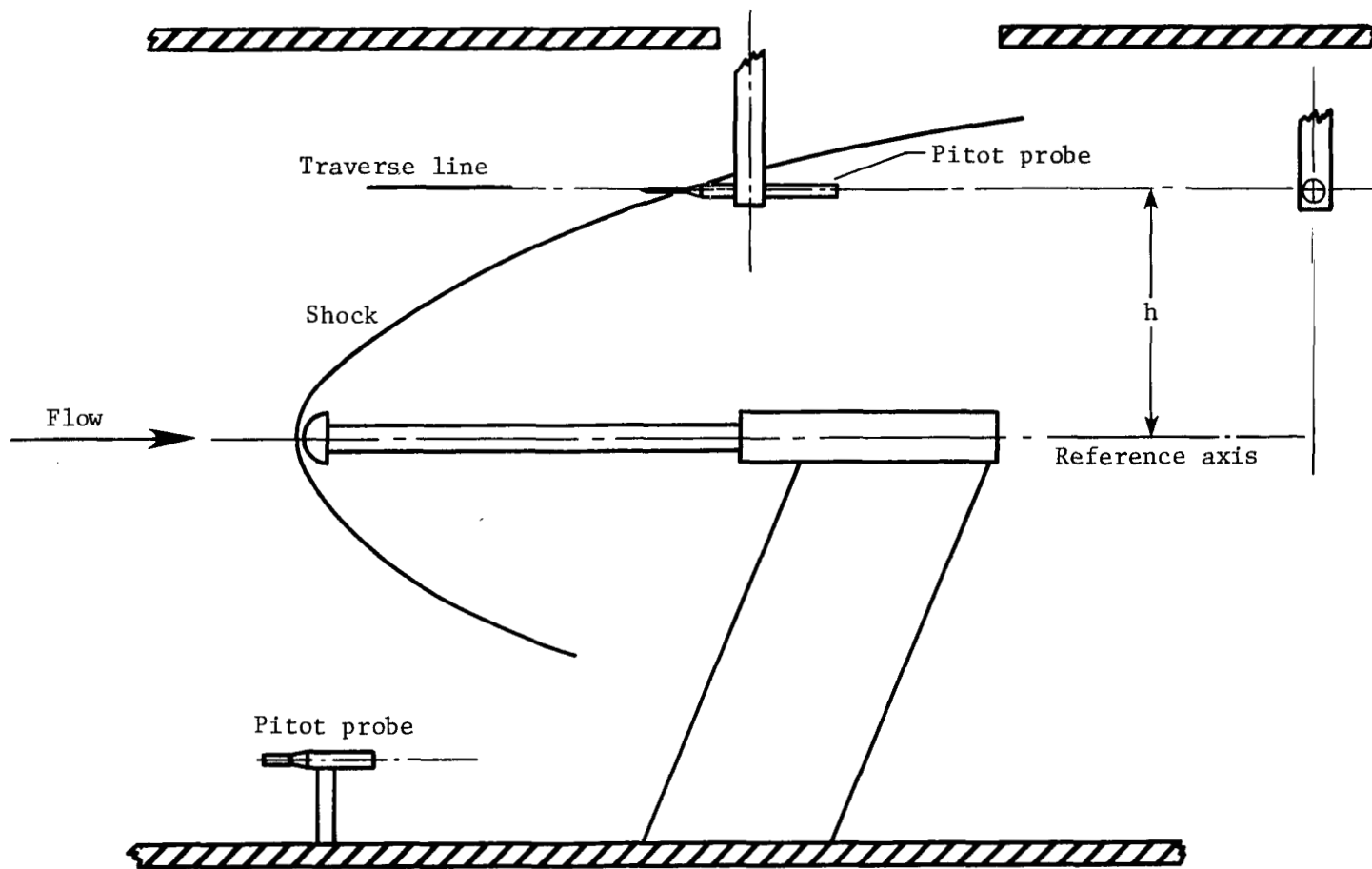


Figure 2.- Schematic of test setup.

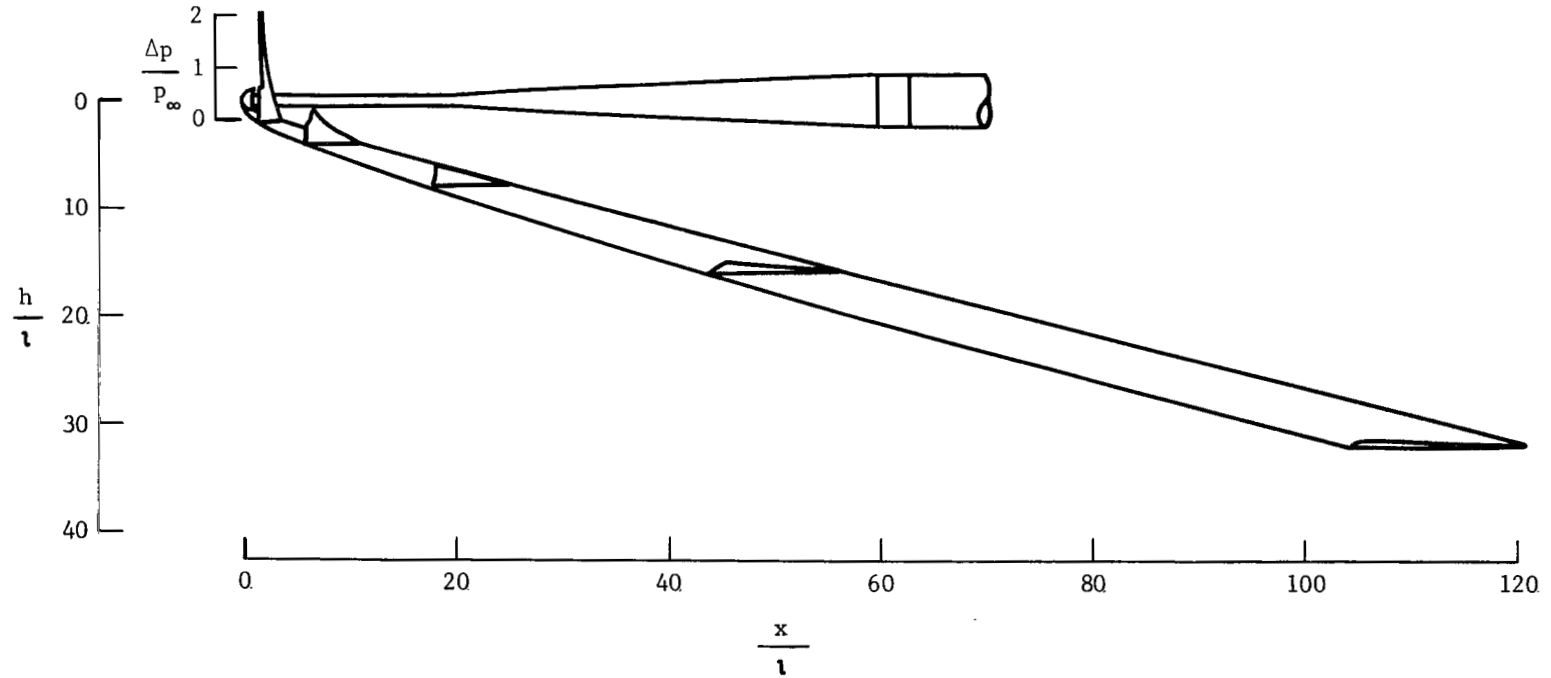
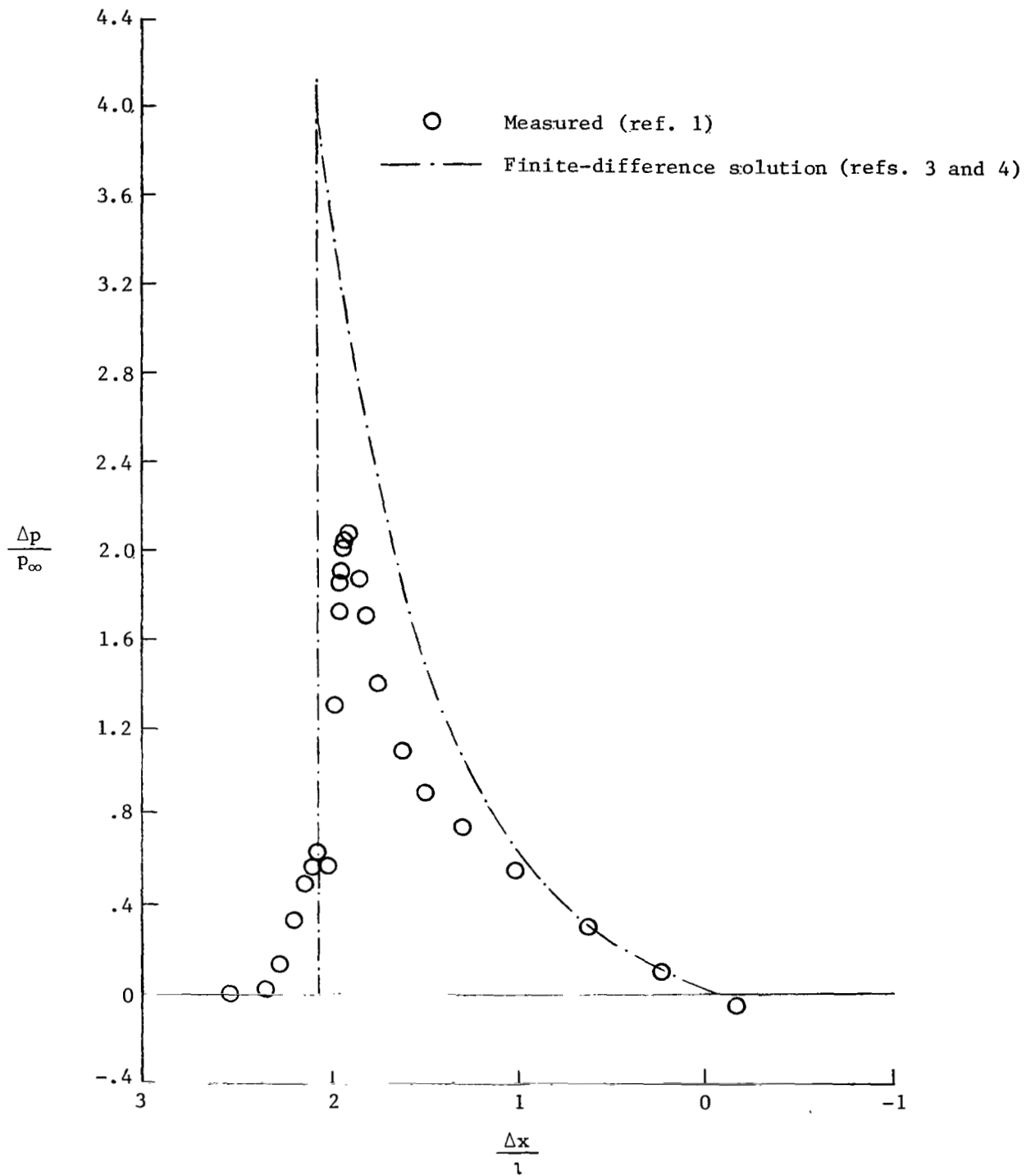
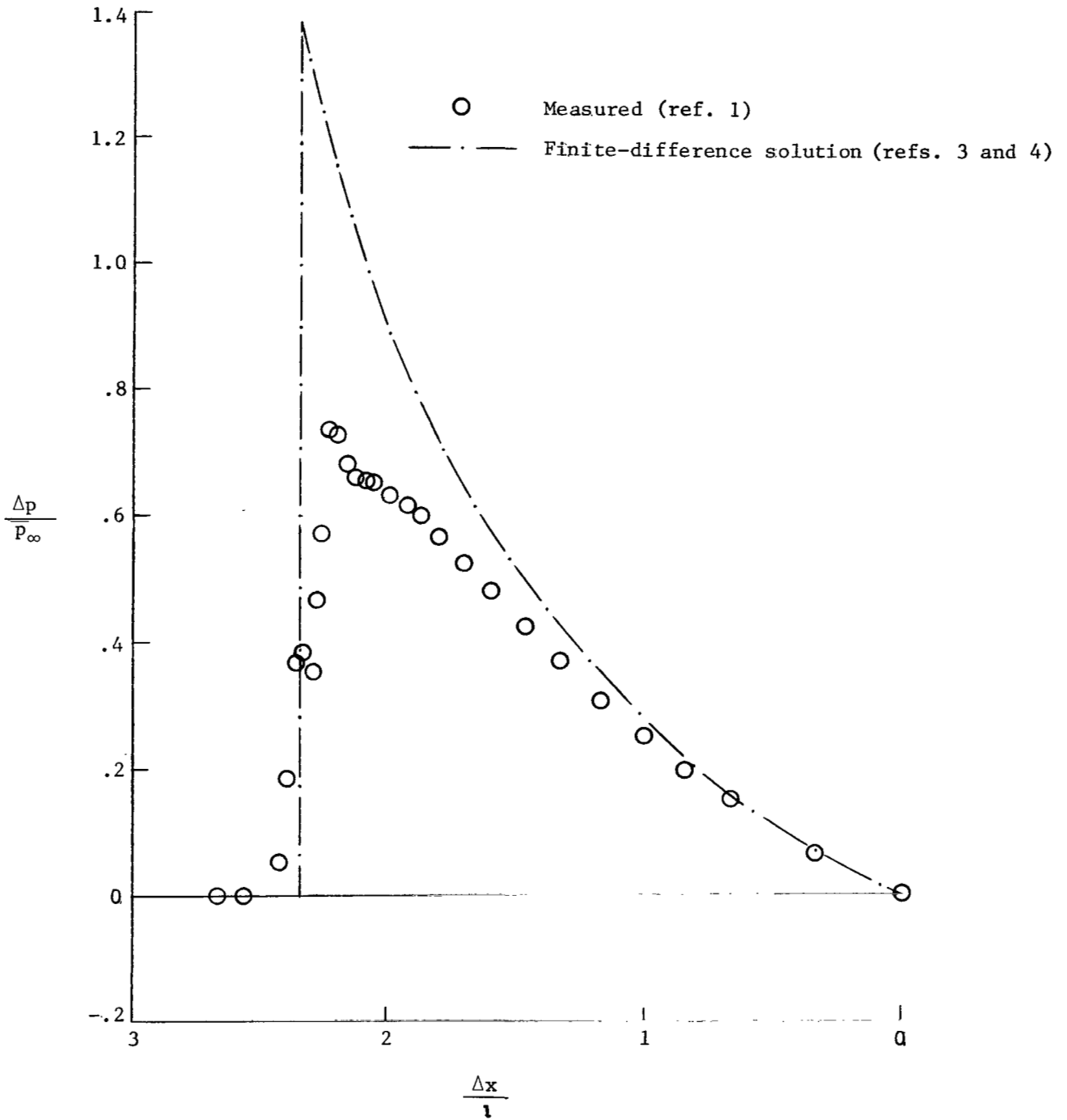


Figure 3.- Scaled pictorial representation of model pressure field at  $M_\infty = 4.14$  (ref. 1).



(a) Large model;  $h/l = 2$ .

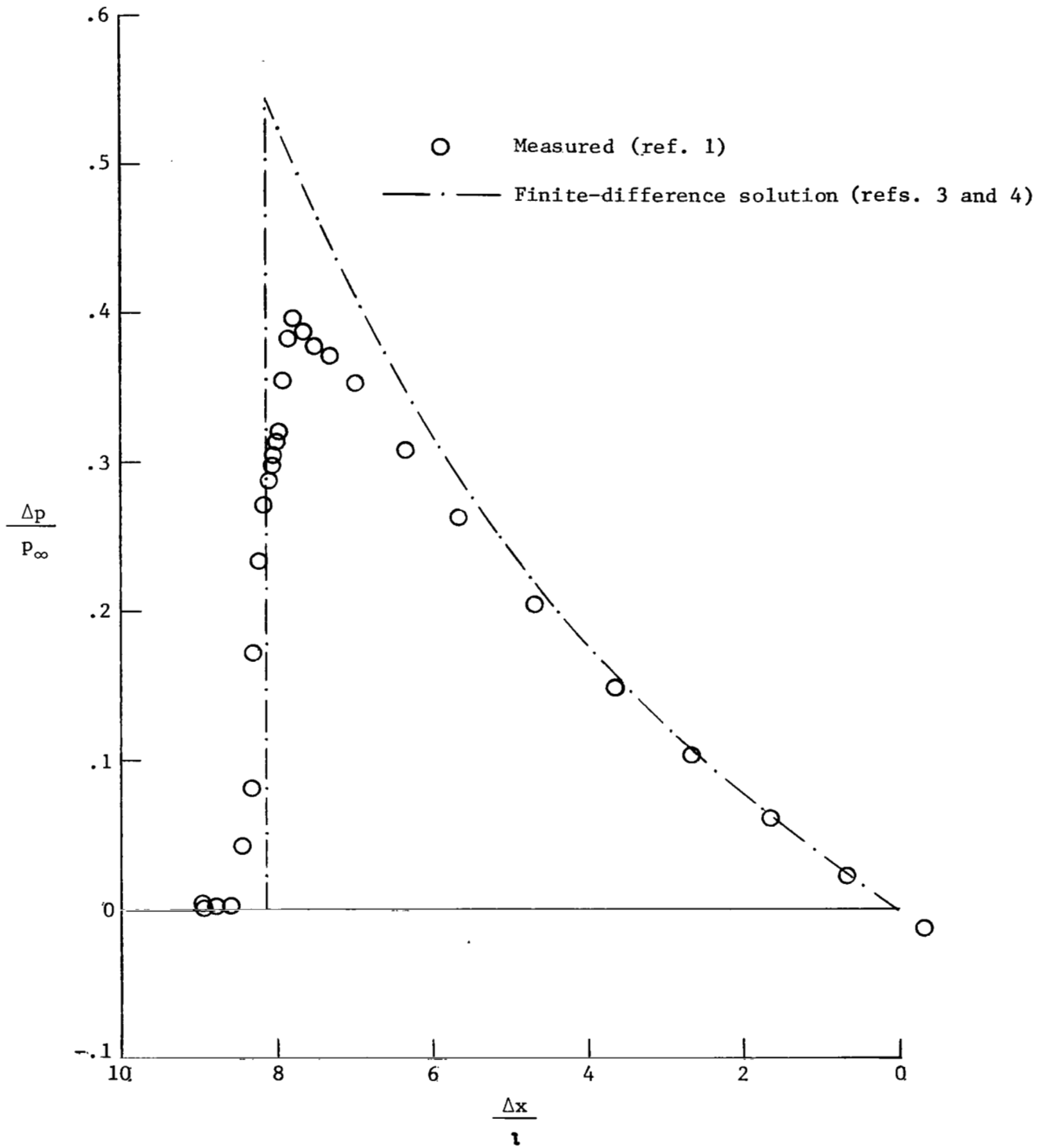
Figure 4.- Comparison of measured (static pressure probe) and calculated signatures at various distances for  $M_\infty = 4.14$ .



(b) Large model;  $h/l = 4$ .

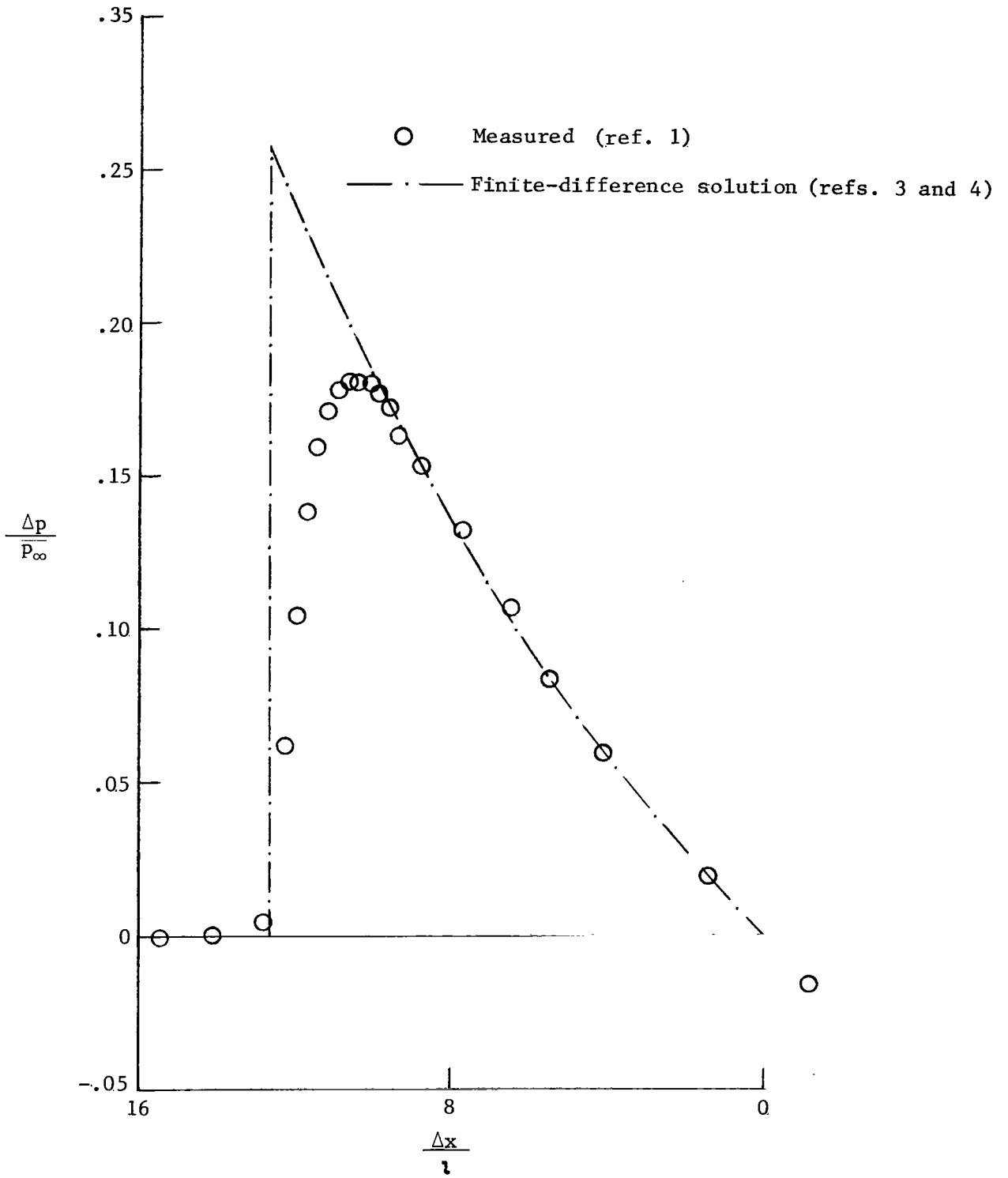
Figure 4.- Continued.





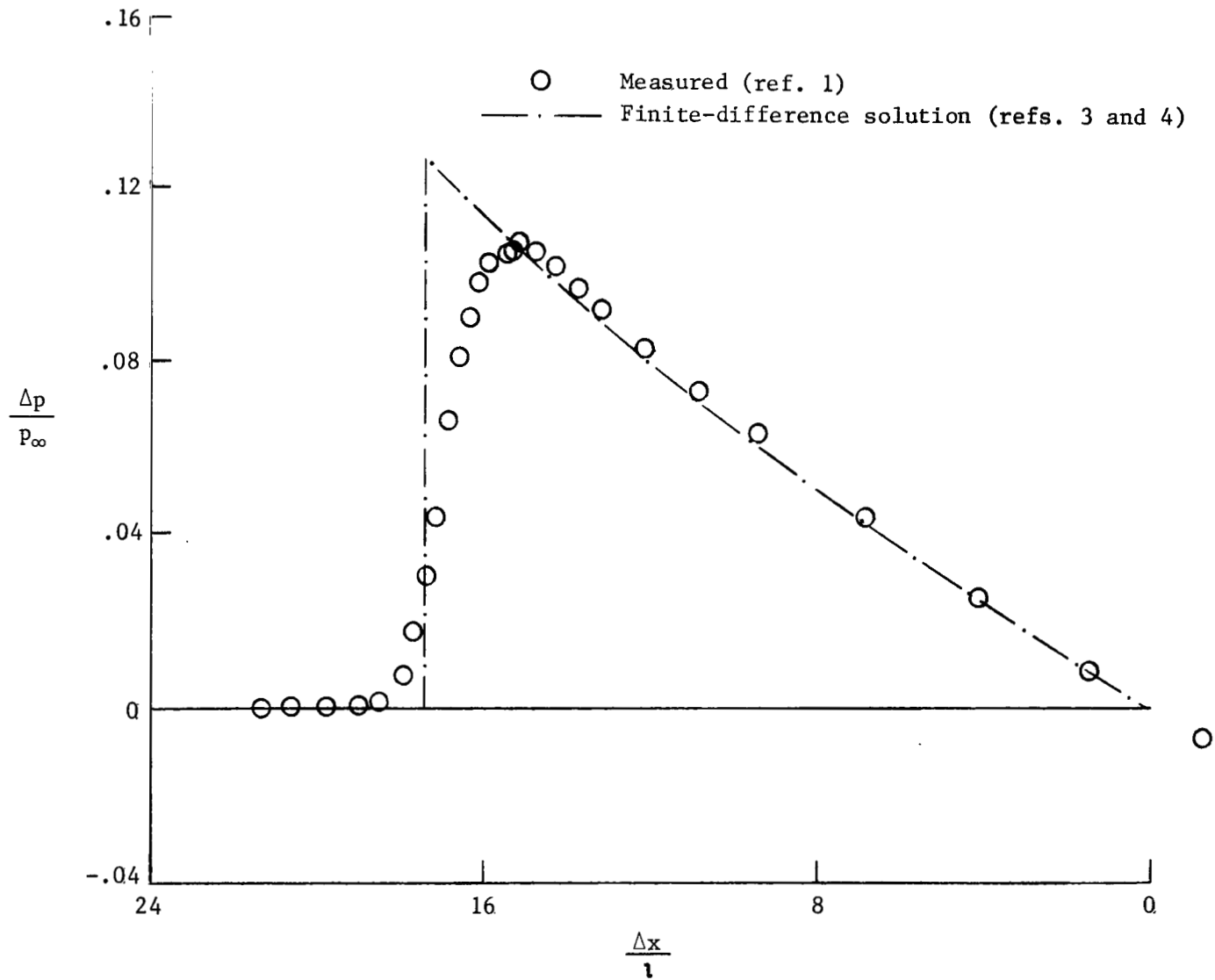
(c) Large model;  $h/l = 8$ .

Figure 4.- Continued.



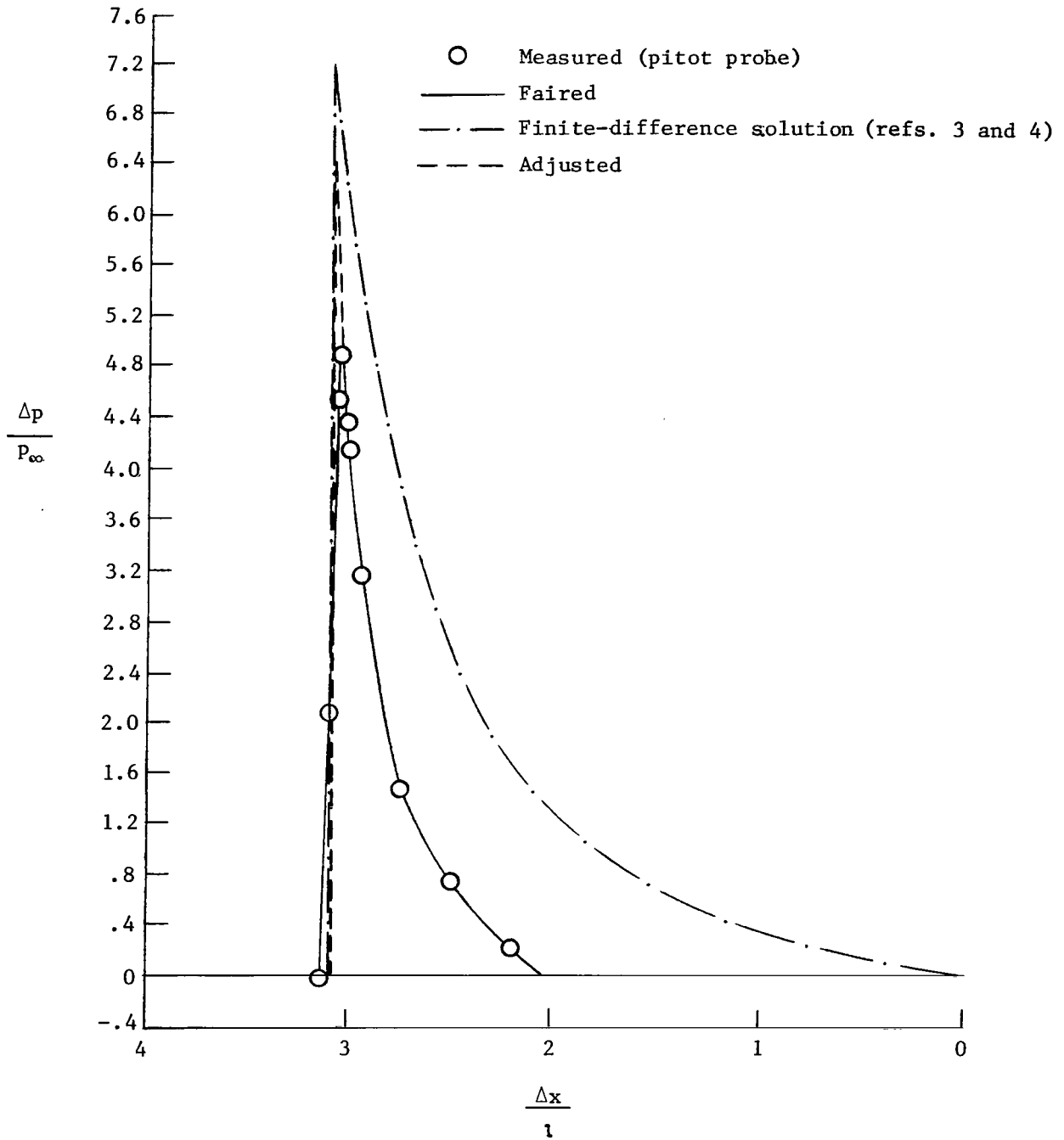
(d) Small model;  $h/l = 16$ .

Figure 4.- Continued.



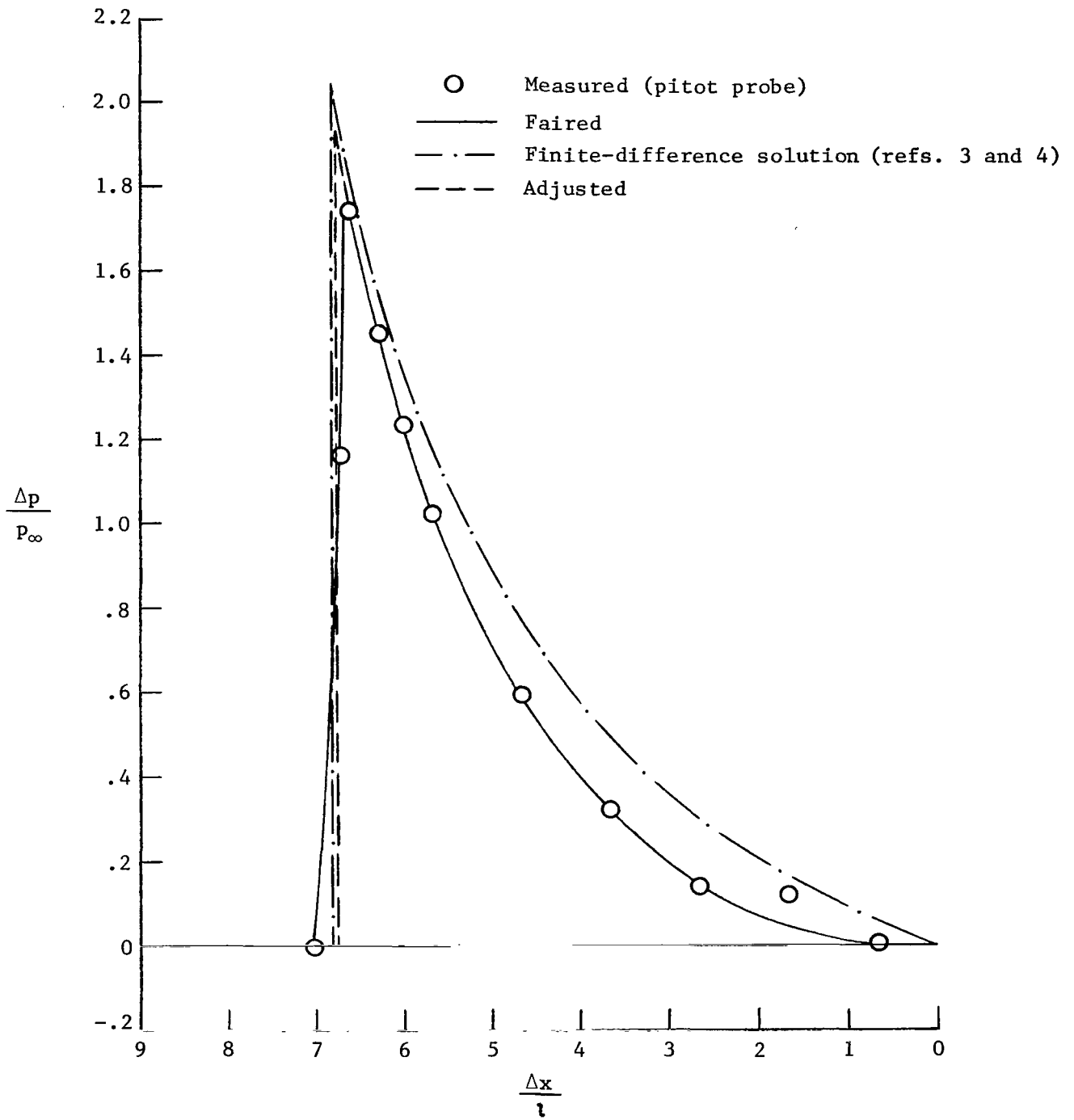
(e) Small model;  $h/l = 32$ .

Figure 4.- Concluded.



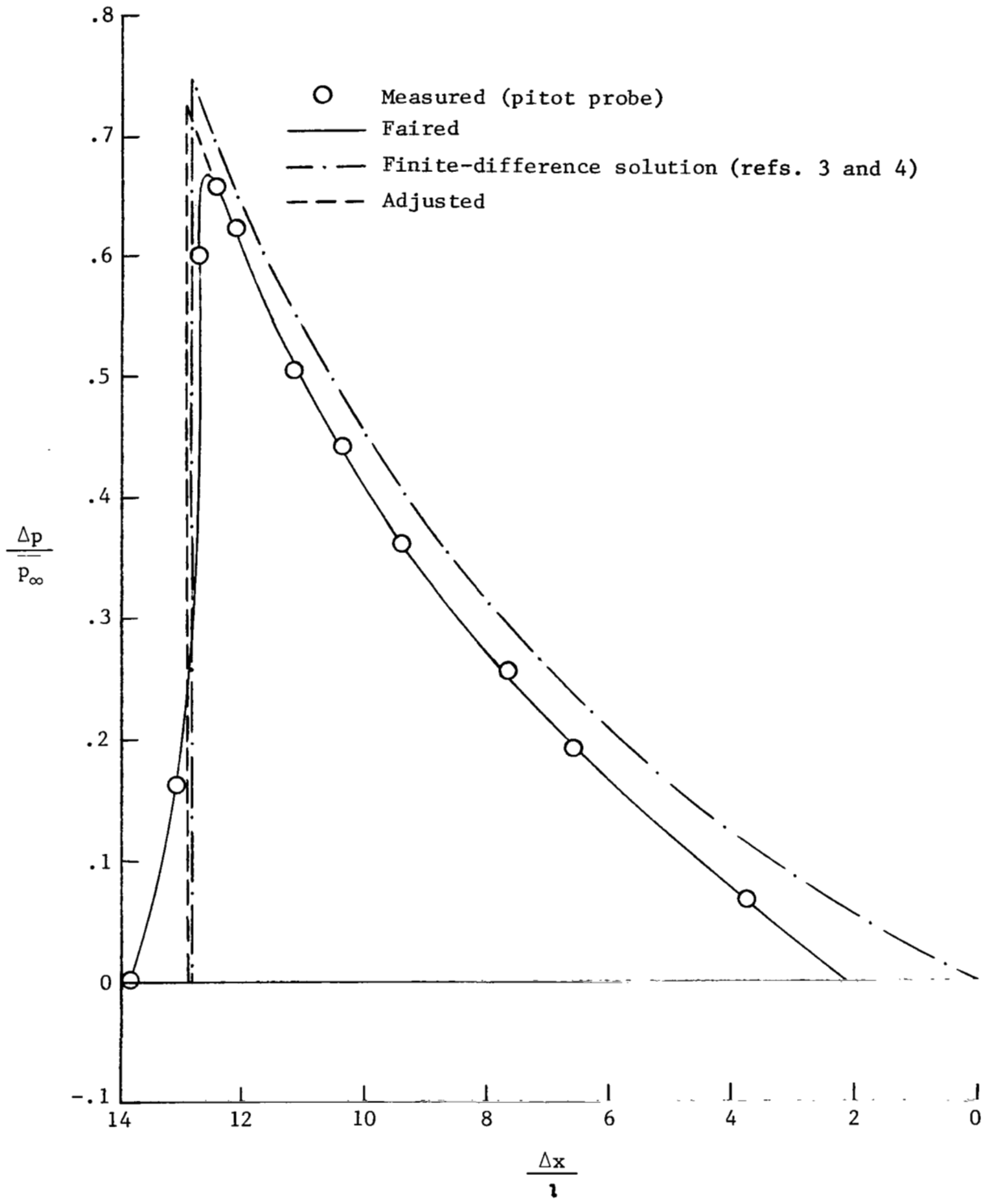
(a) Large model;  $h/l = 2$ .

Figure 5.- Comparison of measured and calculated signatures at various distances for  $M_\infty = 6.0$ .



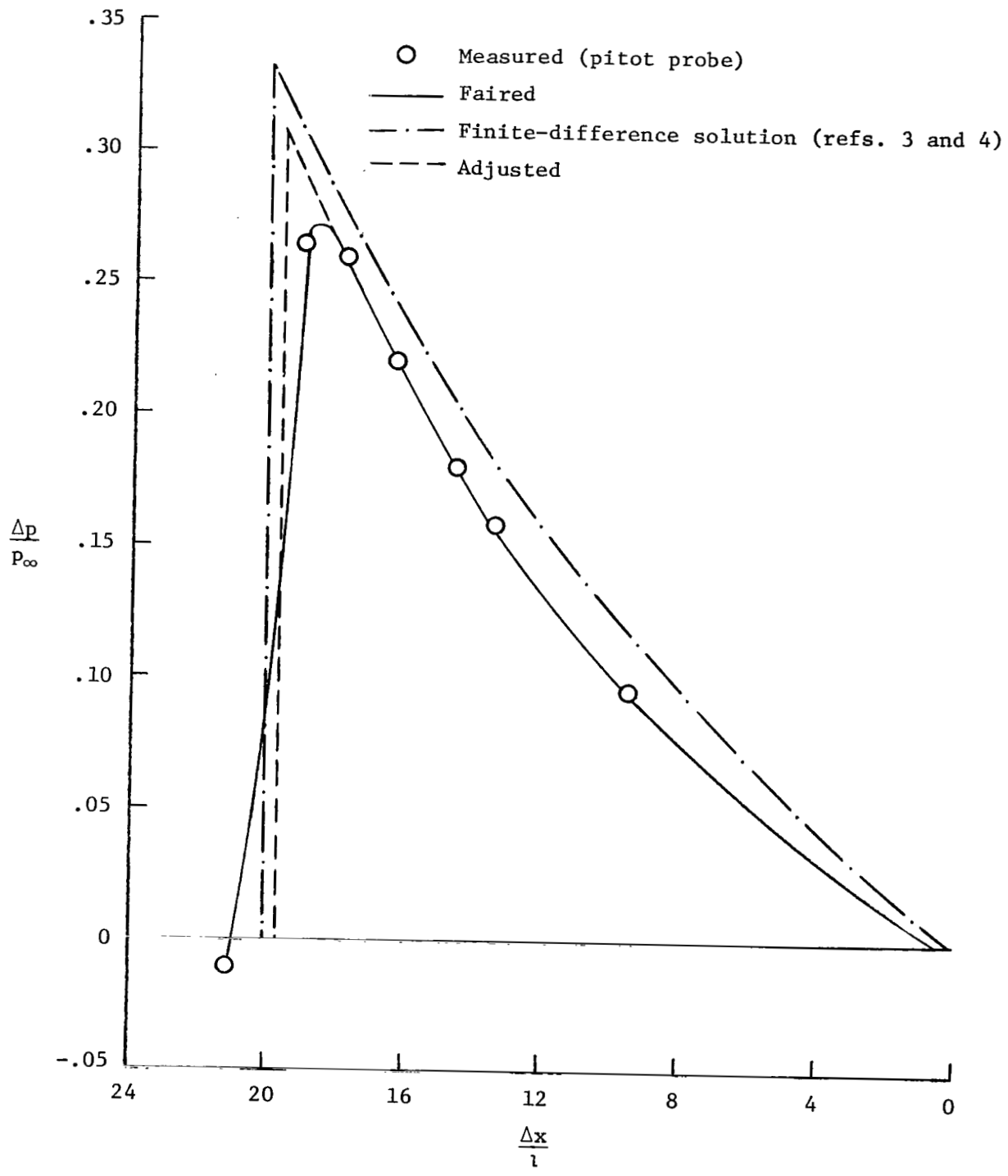
(b) Large model;  $h/l = 4$ .

Figure 5.- Continued.



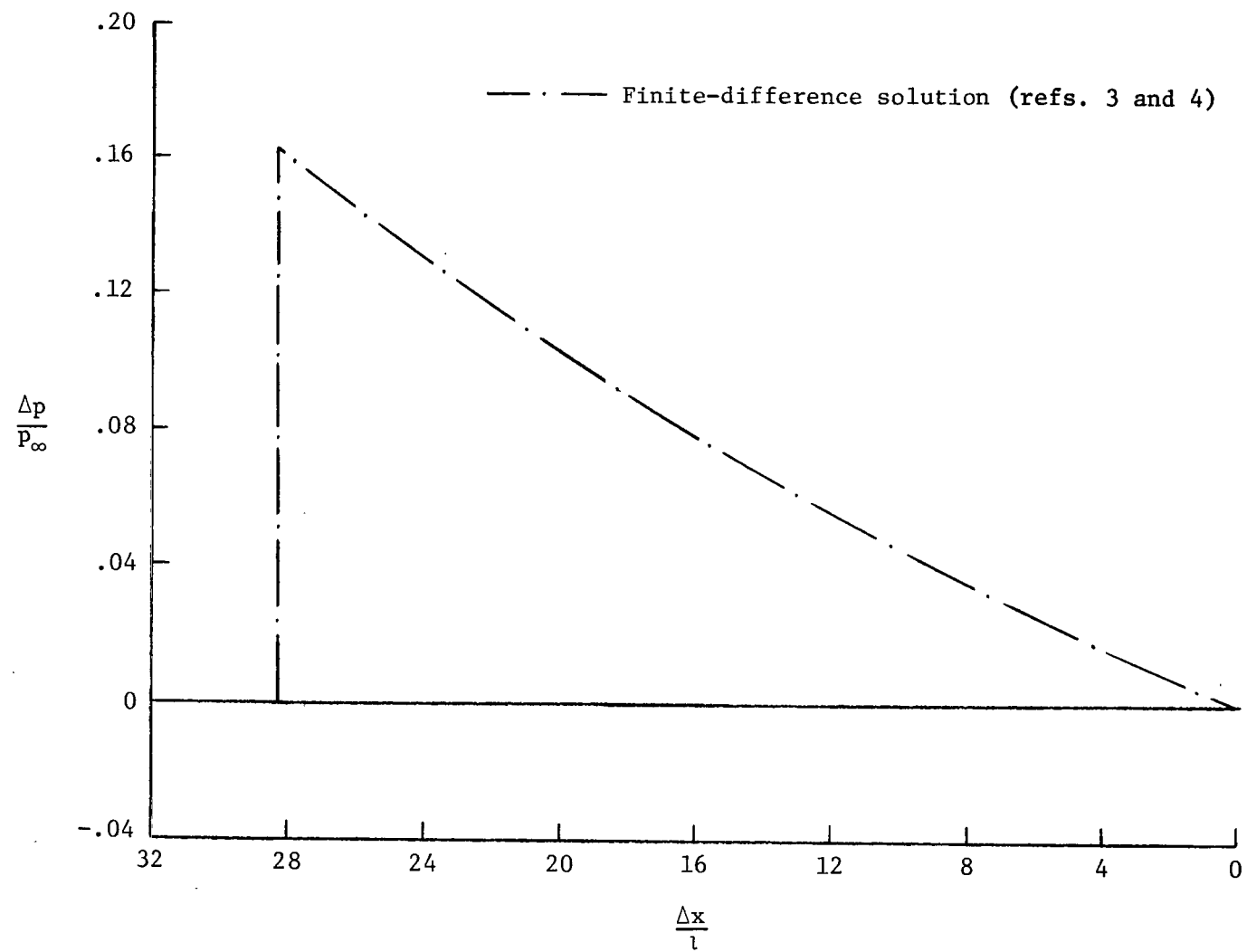
(c) Small model;  $h/l = 8$ .

Figure 5.- Continued.



(d) Small model;  $h/l = 16$ .

Figure 5.- Continued.



(e) Small model;  $h/l = 32$ .

Figure 5.- Concluded.



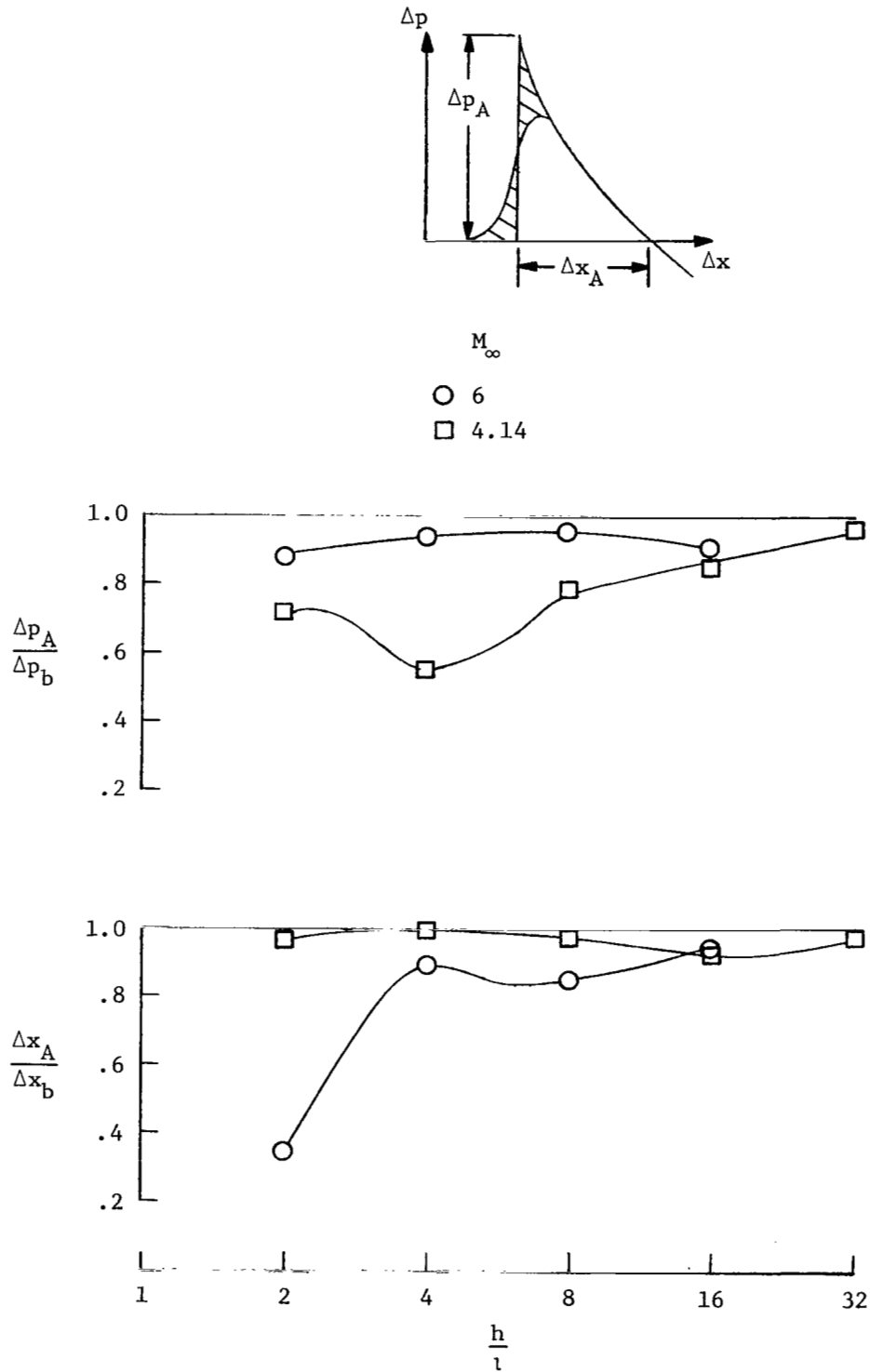


Figure 6.- Variation of the ratios of adjusted signature-parameters, to the calculated signature parameters with distance from the body at Mach numbers 4.14 and 6.

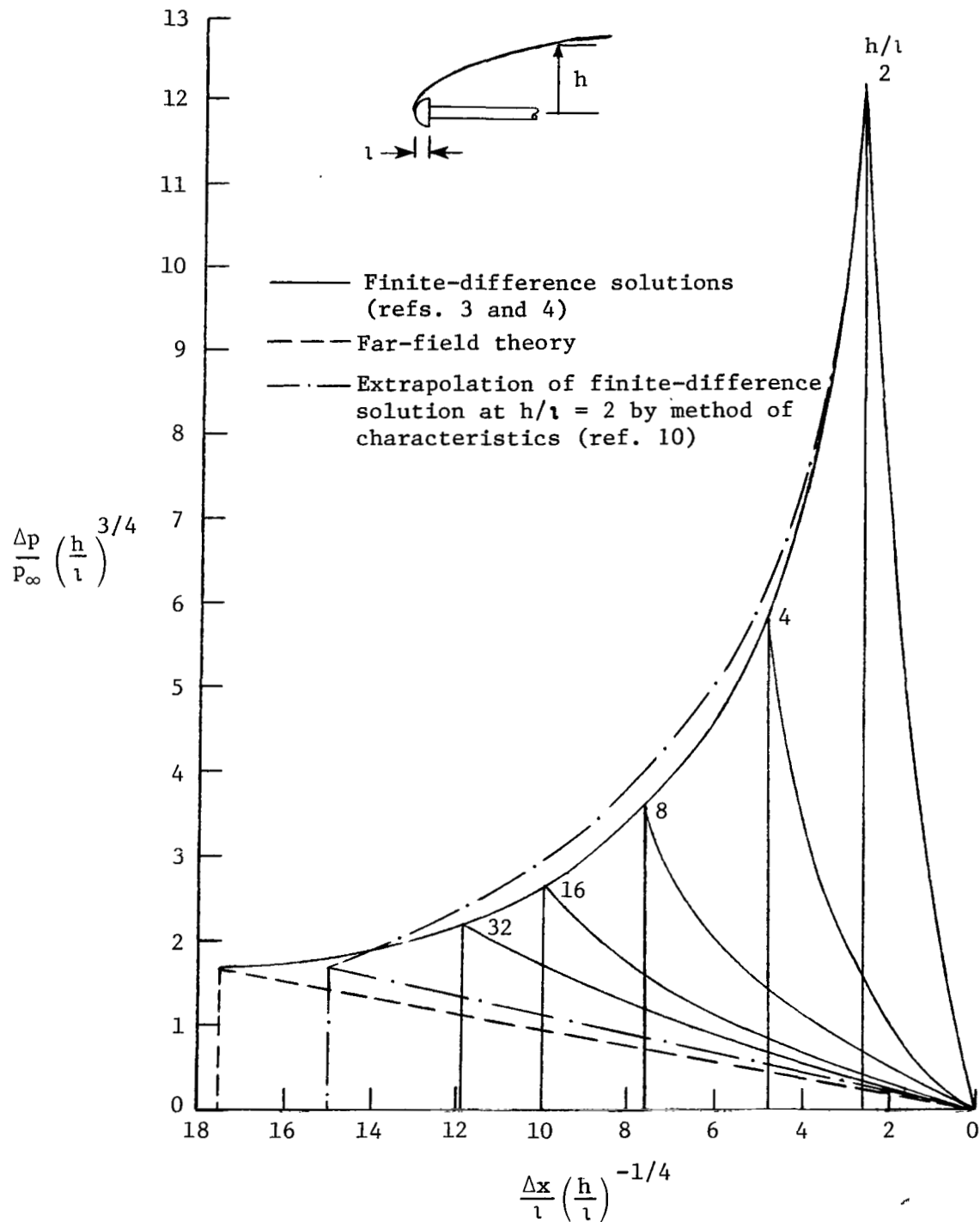
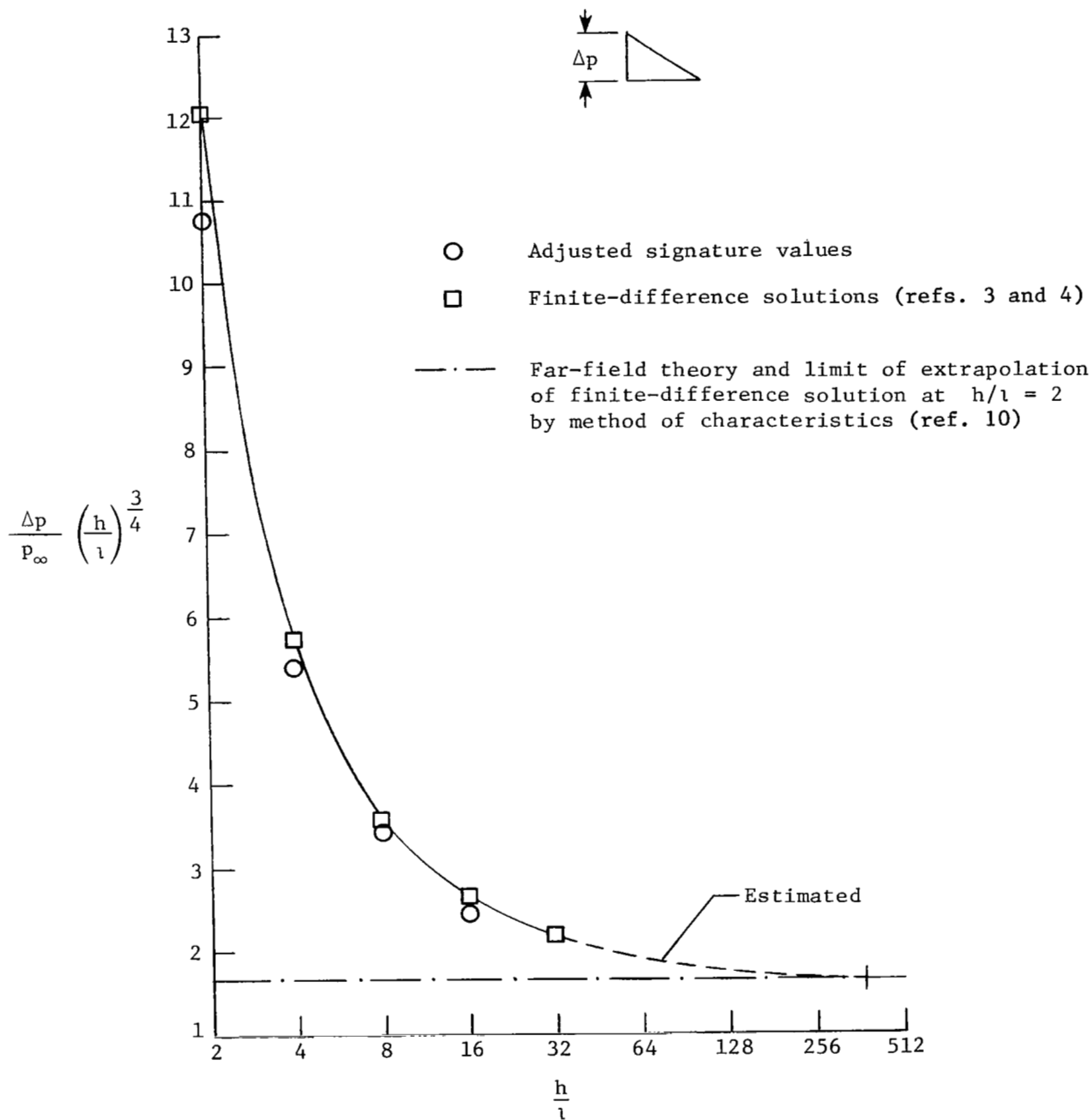
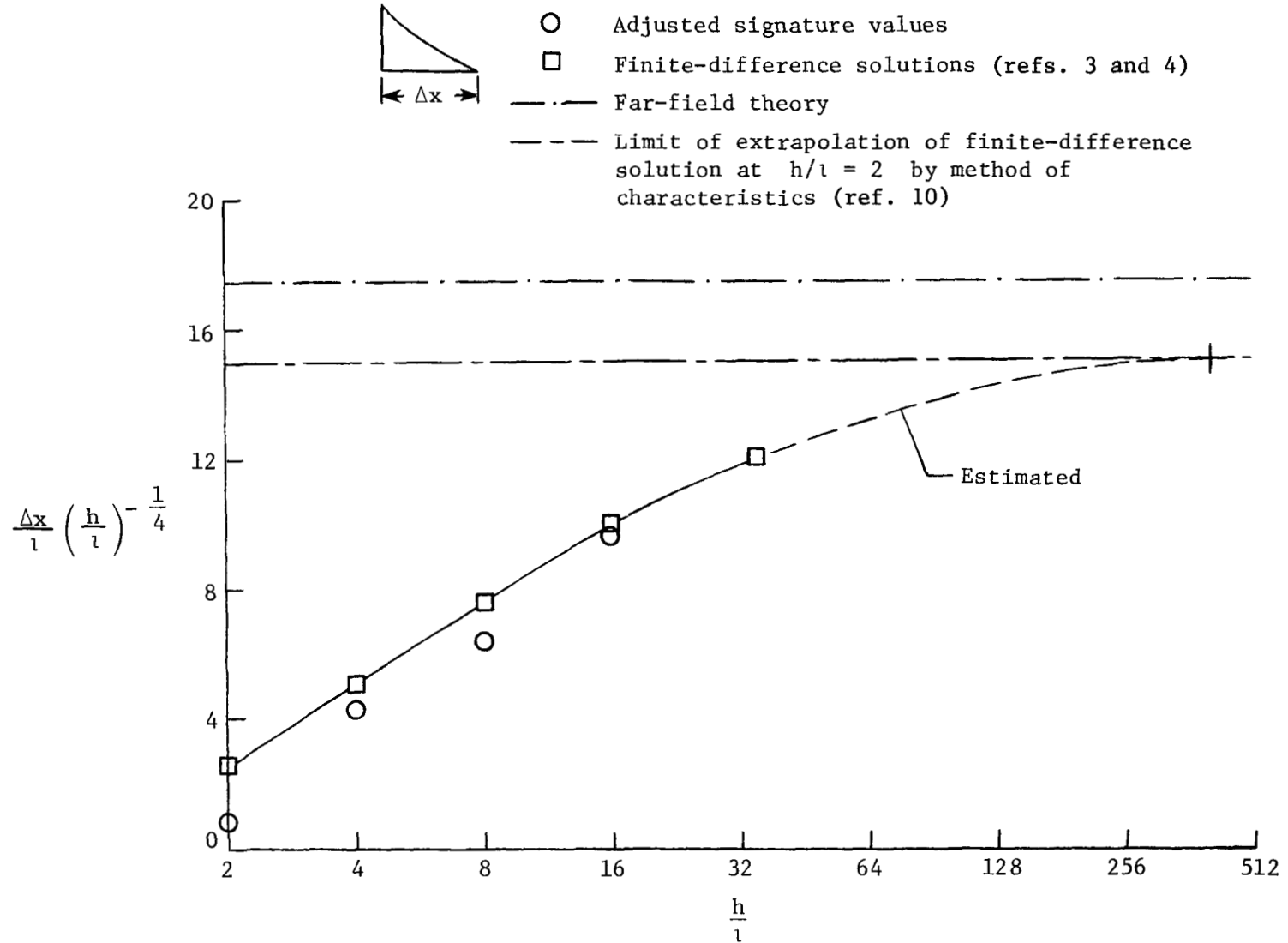


Figure 7.- Calculated signatures in far-field parametric form at  $M_\infty = 6$ .



(a) Peak overpressure.

Figure 8.- Variation of calculated and measured far-field signature parameters with distance at  $M_\infty = 6$ .



(b) Length.

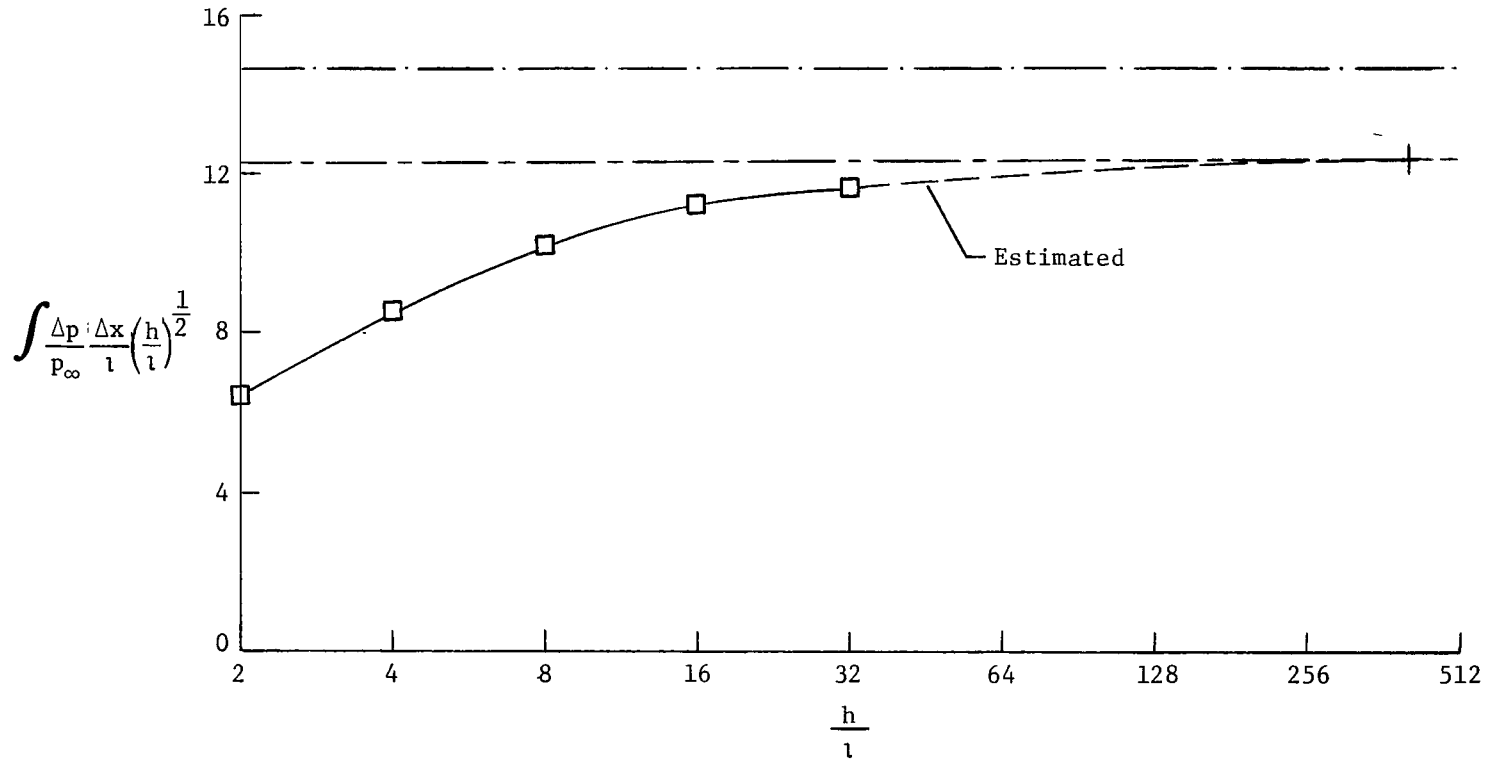
Figure 8.- Continued.

$$\int \frac{\Delta p}{P_\infty} \frac{\Delta x}{l}$$

□ Finite-difference solutions (refs. 3 and 4)

— · — Far-field theory

--- Extrapolation of finite-difference solution at  $h/l = 2$  by method of characteristics (ref. 10)



(c) Impulse.

Figure 8.- Concluded.

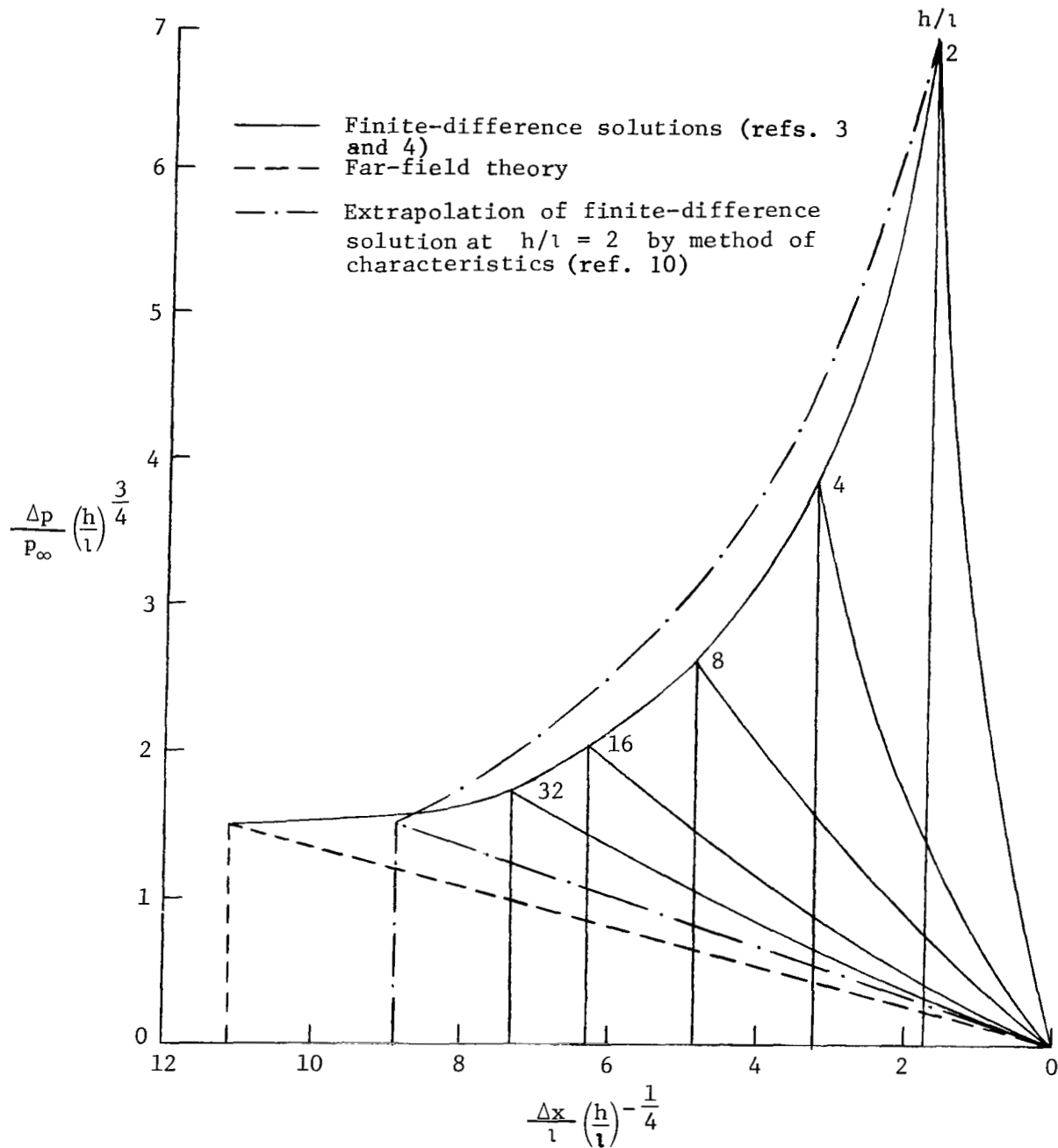
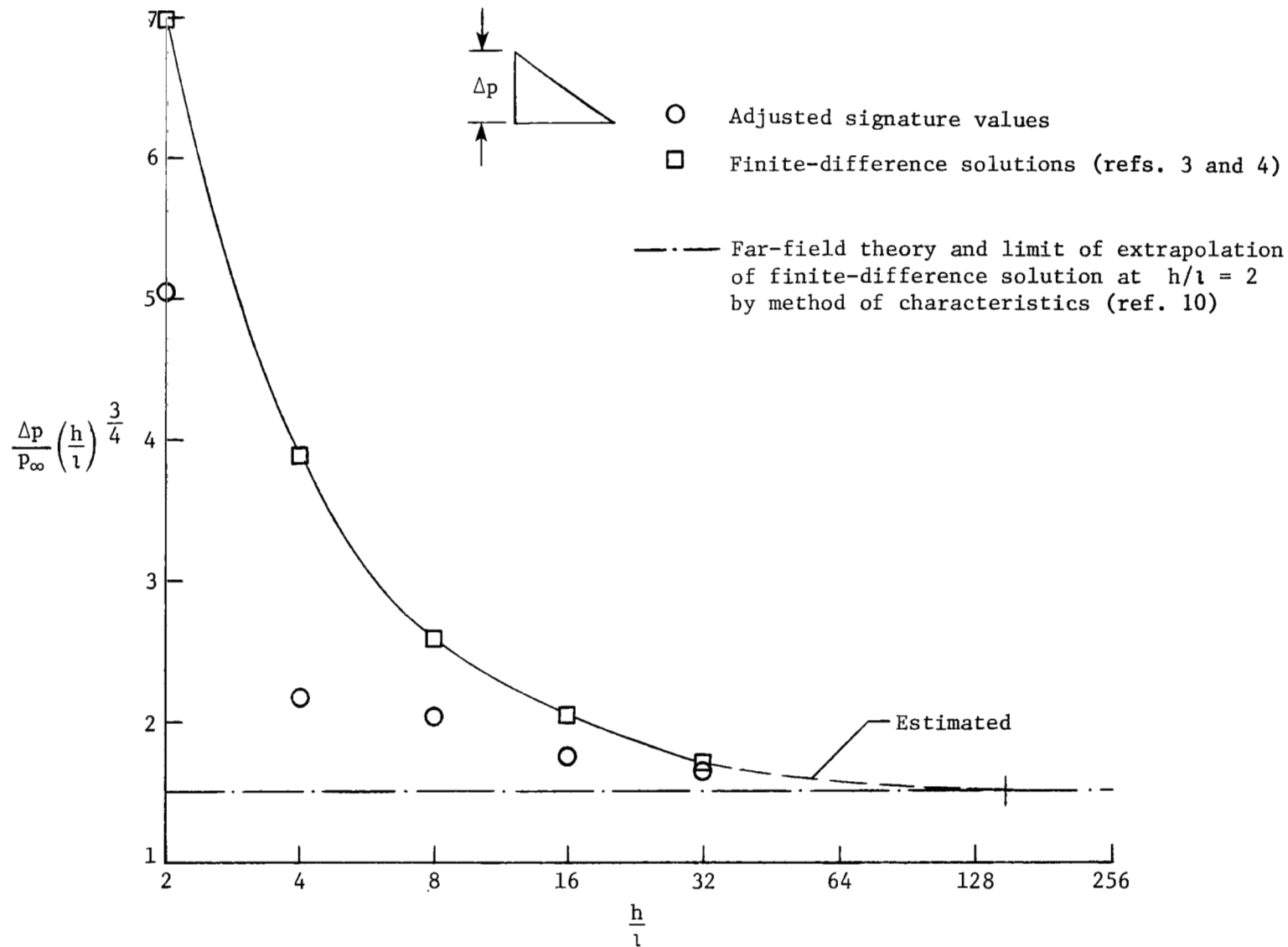
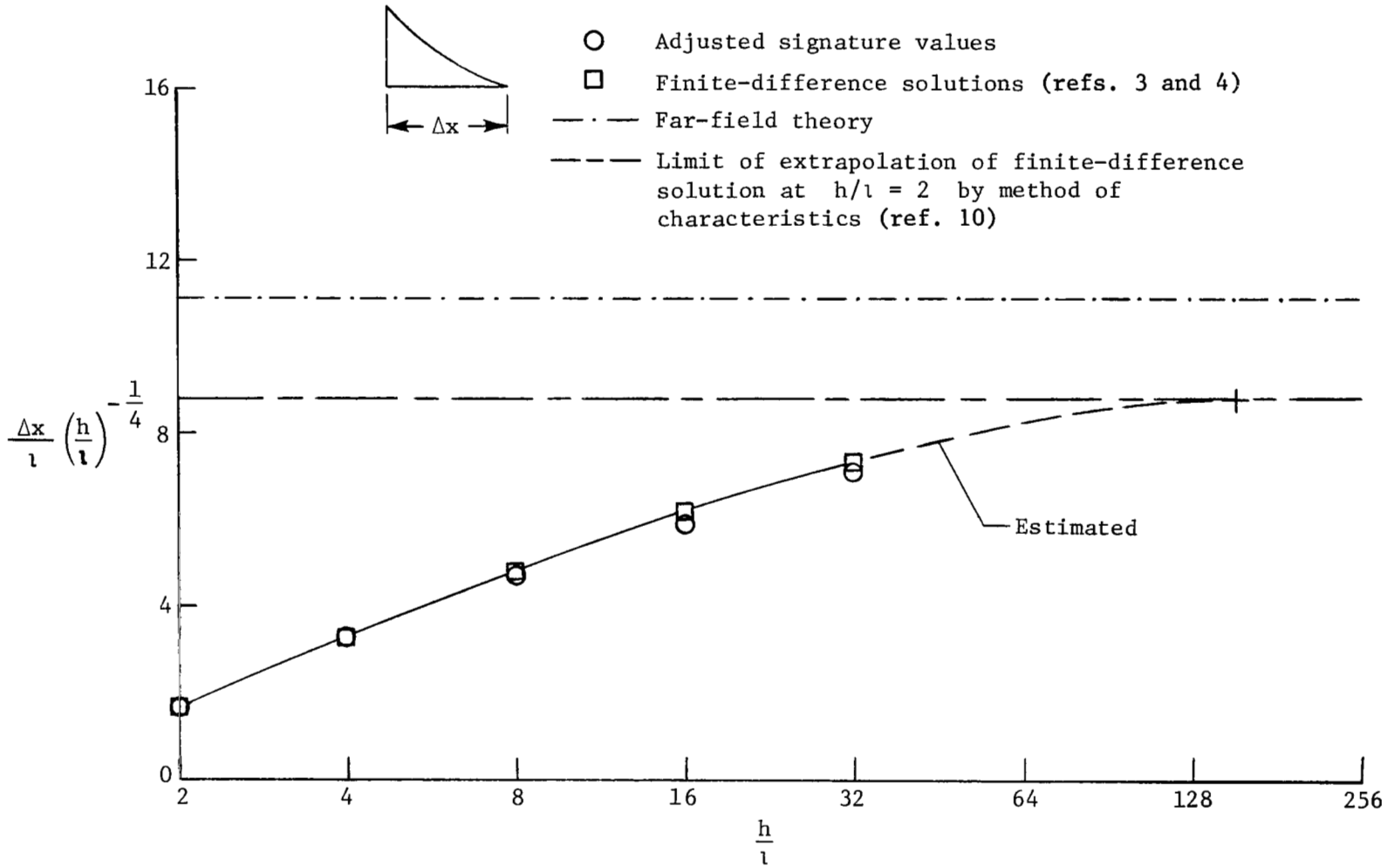


Figure 9.- Calculated signatures in far-field parametric form at  $M_\infty = 4.14$ .



(a) Peak overpressure.

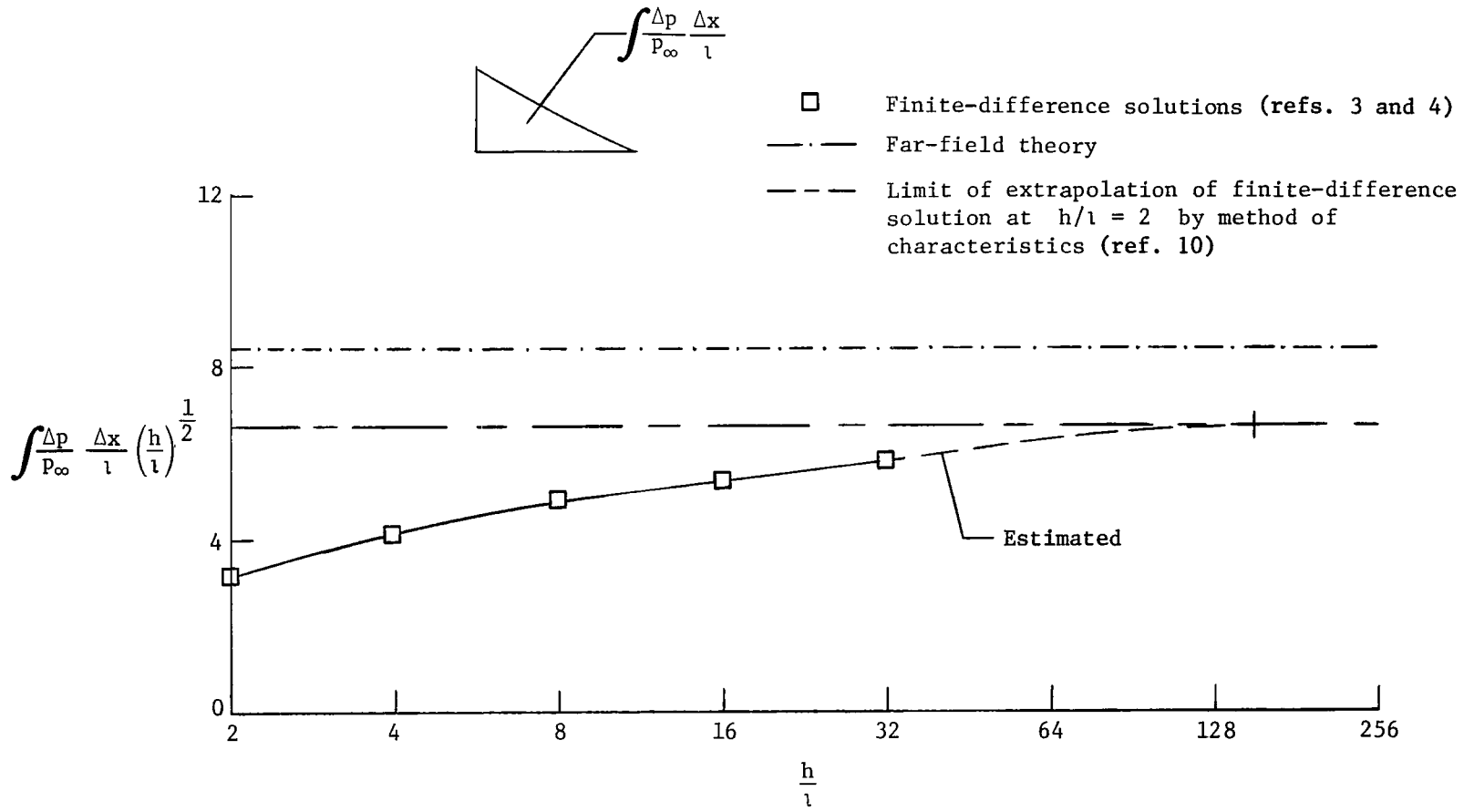
Figure 10.- Variation of calculated and measured far-field signature parameters with distance at  $M_\infty = 4.14$ .



(b) Length.

Figure 10.- Continued.





(c) Impulse.

Figure 10.- Concluded.

1. Report No. NASA TP-1787		2. Government Accession No.		3. Recipient's Catalog No.	
4. Title and Subtitle A STUDY OF THE SONIC-BOOM CHARACTERISTICS OF A BLUNT BODY AT A MACH NUMBER OF 6		5. Report Date December 1980		6. Performing Organization Code 506-51-13-02	
7. Author(s) George C. Ashby, Jr.		8. Performing Organization Report No. L-14017		10. Work Unit No.	
9. Performing Organization Name and Address NASA Langley Research Center Hampton, VA 23665		11. Contract or Grant No.		13. Type of Report and Period Covered Technical Paper	
12. Sponsoring Agency Name and Address National Aeronautics and Space Administration Washington, DC 20546		14. Sponsoring Agency Code		15. Supplementary Notes	
16. Abstract An experimental and analytical study of the sonic-boom static-pressure signatures generated by a blunt body at Mach 6 has shown that finite-difference computer programs can be used to give reasonable estimates of the signatures. The calculated near-field static-pressure signature was extrapolated to the far field by a program using the method of characteristics. A comparison of this extrapolated signature with the signature predicted by far-field sonic-boom theory (linearized) shows that peak overpressures are about the same, at least up to Mach 6, but the far-field theory overestimates the length of the signature.					
17. Key Words (Suggested by Author(s)) Blunt bodies Hypersonic Sonic boom			18. Distribution Statement Unclassified - Unlimited		
19. Security Classif. (of this report) Unclassified		20. Security Classif. (of this page) Unclassified		21. No. of Pages 31	22. Price A03
				Subject Category 01	

National Aeronautics and  
Space Administration

Washington, D.C.  
20546

Official Business  
Penalty for Private Use, \$300

THIRD-CLASS BULK RATE

Postage and Fees Paid  
National Aeronautics and  
Space Administration  
NASA-451



15 1 1U,A, 121980 S00903DS  
DEPT OF THE AIR FORCE  
AF WEAPONS LABORATORY  
ATTN: TECHNICAL LIBRARY (SUL)  
KIRTLAND AFB NM 87117

**NASA**

POSTMASTER: If Undeliverable (Section 158  
Postal Manual) Do Not Return

---